HOKKAIDO UNIVERSITY

Title	Bubble generation and molecular crystallization at solution surface by intense continuous-wave laser irradiation
Author(s)	Chen, Jim Jui-Kai; Yuyama, Ken-ichi; Sugiyama, Teruki et al.
Citation	Applied Physics Express (APEX), 11(8), 085502 https://doi.org/10.7567/APEX.11.085502
Issue Date	2018-08
Doc URL	https://hdl.handle.net/2115/75094
Rights	© 2018 The Japan Society of Applied Physics
Type	journal article
File Information	Manuscript_for_APEX_(bubble_generation)_for_revision.pdf

Hokkaido University Collection of Scholarly and Academic Papers : HUSCAP

Bubble generation and molecular crystallization at solution surface by intense continuous-wave laser irradiation

Jim Jui-Kai Chen[1], Ken-ichi Yuyama[1,2]*, Teruki Sugiyama[1,3,4]*, and Hiroshi Masuhara[1,3]*

[1]*Department of Applied Chemistry, National Chiao Tung University, Hsinchu 30010, Taiwan*

[2]*Research Institute for Electronic Science, Hokkaido University, Sapporo, Hokkaido 001-0020, Japan*

[3]*Center for Emergent Functional Matter Science, National Chiao Tung University, Hsinchu 30010, Taiwan*

[4]*Division of Materials Science, Graduate School of Science and Technology, Nara Institute of Science and Technology, Ikoma, Nara 630-0192, Japan*

E-mail: yuyama@es.hokudai.ac.jp, sugiyama@g2.nctu.edu.tw, masuhara@masuhara.jp

We demonstrate bubble generation outside the focus induced by irradiating a focused 1064-nm continuous-wave laser beam into surface of water and L-phenylalanine H_2O solution. In the former case of water, bubbles stay at positions distant from the focus during the irradiation, and their size and location are controllable by laser power. In the latter solution, bubbles move toward the surrounding, and subsequently crystallization takes place at the focus. We discuss these behaviors from the viewpoints of temperature elevation accompanying the decrease in air solubility as well as of optical trapping of L-phenylalanine clusters giving a single crystal.

Optical trapping with a tightly focused continuous-wave (cw) laser beam has been widely employed as optical tweezers for trapping small objects with the size ranging from micrometer to nanometer in solution.[1] In the past decade, we have intensively explored new optical trapping phenomena in molecular and colloidal solutions at their interface.[2–5] We succeeded in inducing crystallization of amino acids by irradiating a 1064-nm cw laser beam at solution surface.[2] Intense laser irradiation into solution surface leads to local concentration increase through optical trapping of liquid-like clusters, in which solute and solvent molecules are weakly linked, and eventually crystal nucleation takes place at the focus. In L-phenylalanine (L-Phe) H_2O unsaturated solution, a formed plate-like crystal grows continuously under optical trapping, and its two-dimensional growth rate is controllable by laser power.[3] In optical trapping at surface of colloidal solution, polystyrene nanoparticles of 200 nm in diameter form a disk-like assembly that shows structural color.[4] Furthermore, optical trapping of 500-nm polystyrene nanoparticles at glass/solution interface gives a colloidal assembly that expands into non-irradiated area with sticking out aligned particles like horns.[5]

Through the systematic study on optical trapping at interface, we accidentally found that bubbles are generated outside the focus upon irradiation of the high intensity 1064-nm cw laser at solution surface of pure H_2O and L-Phe H_2O solution. Bubble generation phenomena are frequently reported under irradiation of a focused cw laser into photo-absorbers.[6–13] A single vapor microbubble is generated at the focus, and the nanometer-sized objects are attracted to the bubble by the fluidic force. Based on these characteristics, the cw-laser induced bubble generation has been applied to manipulation of DNA[6], crystallization of glycine[7], and patterning of quantum-dots[8], carbon nanotubes[9], and micro-particles[10]. The bubble generation in this Letter is quite different from these previous studies. Firstly, multiple bubbles are generated outside the focus. Secondly, bubbles appear after a while from the beginning of the irradiation. Thirdly, bubbles are stably located at positions distant from the focus, and their location is controllable by changing laser power. We show this unique bubble generation dynamics and discuss its possible mechanism, which provides important information on laser trapping-induced crystallization of amino acids.

Laser irradiation and optical microscopic observation were carried out with an inverted

microscope (supplementary data). Figure 1 shows a series of optical micrographs captured with a charge-coupled device (CCD) video camera during laser irradiation at 1.1 W into surface of a water thin film of 15 μL. At the beginning, we observed only a small bright spot ascribed to light reflection at water surface. At about 120 sec, two circular rings of 20 μm diameter appeared from lower position of the image (Fig. 1a). The edge of two rings gradually became darker and clearer, while they came close to the focus (Fig. 1b). Eventually, two rings reached positions 50 μm distant from the focus and stayed there stably for subsequent 40 sec. During this period, two rings were located at the almost same positions with small fluctuation, and the distance between the centers of the rings and the focus was kept nearly constant. It is reasonable to consider that the two rings are bubbles because the sample was pure water, namely, no molecule, nano- and micro-particle was added, they were prepared only by intense laser irradiation and disappeared upon its switching off. Their shape is always spherical, which is ascribed to surface tension. The initial optical micrograph giving pale rings implies that bubbles are located outside the focal plane. Namely, we infer that bubbles are possibly generated inside the water thin film and gradually move up to water surface at which the focus was set.

At 170 sec, new two bubbles appeared (Fig. 1c). The bubbles moved close to the focus with accompanying the change in the contrast, while the initially formed bubbles were stably located around the focus. Eventually, the newly generated two bubbles arrived at positions 50 μm distant from the focus (Fig. 1d). The video movie of the bubble generation is uploaded as supplementary data. It should be noted that the size and the distance from the focus was nearly identical among four bubbles during laser irradiation. This steady state was kept for more than 1000 sec (Fig. 1e).

The line profile for one bubble observed at 1205 sec is shown as the inset in the corresponding image (Fig. 1e). The bubble size that was defined here as the largest diameter of the dark ring was estimated to 26 μm at this time. When laser power was decreased down to 0.5 W, four bubbles came close to the focus. The bubbles decreased in their size down to 19 μm during their movement and finally arrived at positions 30 μm distant from the focus (Fig. 1f). When laser power was increased, the bubbles went away from the focus, and their size became larger gradually. At 0.8 W, the bubbles of 23 μm in their size stayed at positions 45 μm distant from the focus (Fig. 1g). At 1.1 W, the bubble

size and the distance from the focus were estimated to 27 μm and 50 μm, respectively (Fig. 1h). Thus, the bubble size and the distance from the focus could be controlled by laser power.

Bubbles were always observed after a few minutes from the beginning of the irradiation. The number of bubbles was different among samples, and the maximum value was 4 under the 1.1-W irradiation in water. The bubbles were kept stably during laser irradiation; however, they quickly disappeared after switching off the laser. The bubble disappearance dynamics was examined by an electron multiplying CCD (EMCCD) camera synchronized with a shutter to cut off the laser. A bubble was observed as a dark circle in the transmission image during laser irradiation (Fig. 2a). This is because illumination light is scattered by the bubble and intensity of light passing through the bubble becomes weak compared to the surrounding solution. The initial bubble diameter just before turning off the laser was about 15 μm, which was considered to the inner diameter of the dark ring observed in the CCD camera. After switching off the laser, the bubble was continuously extended with time, and its size attained to 20 μm at 48 msec (Fig. 2b). Then the bubble completely disappeared in the image, and its lifetime was estimated to 48 msec.

In order to discuss the role of temperature elevation under laser irradiation, we examined the effect of addition of D_2O on the bubble generation. Ito *et al.* reported that the focused 1064-nm laser irradiation into H_2O elevates temperature in the focal volume through light absorption due to overtone of OH vibrational mode.[14)] The elevation is estimated to 22 K/Watt. On the other hand, this temperature elevation is suppressed to 2.6 K/Watt in D_2O. We prepared H_2O/D_2O mixtures with the D_2O volume ratios of 0, 20, and 100% and carried out the irradiation experiments for 12 samples at each ratio. The bubble generation probabilities in the respective solutions were 83, 66.7, and 0%. The probability became low with the increase in the D_2O content. Thus, light absorption and subsequent temperature elevation are critical for the bubble generation.

The bubble generation in the L-Phe H_2O solution provides important information on laser trapping-induced crystallization. In the L-Phe H_2O solution with saturation degree of 0.58, the generation probability was 28.4% (33 samples), in which the total sample number was 116. Since the probability in the L-Phe H_2O solution was low compared to that in water, L-Phe likely has a role for suppressing the bubble generation. Actually, we

systematically carried out the experiments under the same irradiation condition in the L-Phe H_2O solutions with saturation degree of 0.67–0.92; however no bubble generation was observed in these higher concentration solutions.[3)]

Figure 3 shows a series of optical micrographs of the 80×60 μm^2 area around the focus captured during laser irradiation at 1.1 W into surface of the L-Phe H_2O solution. The field of view was changed to be small compared to the case of Fig. 1, in order to observe the crystallization starting at the focus. Initially, only a small bright spot was observed (Fig. 3a). Four bubbles appeared from the outside of the image and arrived at positions 40 μm distant from the focus (Fig. 3b). The bubbles stably stayed in the almost same positions for several tens seconds and then moved away from the focus (Fig. 3c). The bubbles completely disappeared from the viewing field, and only the focus was observed again (Fig. 3d). Further laser irradiation induced nucleation of an L-Phe plate-like crystal (Fig. 3e). The crystal grew continuously during laser irradiation while being trapped at the focus (Fig. 3f). This crystallization behavior was similar to that in the higher concentration solutions.[3)] The bubble movement and subsequent crystallization were observed for 25 samples. In these samples, we estimated the time at which the bubbles started moving outwardly toward the surrounding. Furthermore, we defined the crystallization time at which a small crystal of a few micrometers is identified in a CCD image. The bubbles started moving at the time of 182–480 sec (Fig. 4a). On the other hand, the crystallization time was 182–1253 sec and much different among samples (Fig. 4b). This is possibly ascribed to stochastic nature of crystal nucleation, as one single crystal was always observed. In most samples, time lag was observed between the bubble movement and the crystallization (Fig. 4c), while several samples showed the crystallization immediately after the bubbles started moving. The remaining 71.6% (83) of the total samples (116) showed only the crystallization without the bubble generation.

Based on the above results, we discuss possible mechanism for the bubble generation (Fig. 5). In conventional experiments on cw laser-induced bubble generation,[6–13)] one bubble is formed at the focus where temperature is increased over the boiling point of solvent through efficient photo-thermal conversion. Namely, a vapor bubble is formed through liquid/gas phase transition. In the present experiments, bubbles are not generated at the focus where temperature should be the highest. Furthermore, we estimated that the

temperature at the focus is 50 °C,[14] which is lower than the boiling point of water. These results imply that bubbles in this study are ascribed not to vapor of water molecules but to air evaporated from water.

Air solubility in water is decreased with the elevation of temperature.[15] When a 1064-nm cw laser beam is irradiated into water, the laser is absorbed in its optical path. Temperature is elevated through photo-thermal conversion due to absorption of the 1064-nm photon by OH vibrational overtone (Fig. 5a). The generated heat is diffused to the surrounding solution, and temperature distribution is widened (Fig. 5b). There air solubility is decreased, and the dissolved air appears as bubbles (Fig. 5c). The bubbles will receive the scattering force in the optical path, because their refractive index is low compared to the surrounding solution. As the result, the bubbles are possibly kicked out from the optical path and move up to water surface due to buoyancy force. The temperature distribution formed through photo-thermal conversion generates surface tension distribution, resulting in convection flow toward the surrounding from the focus. Actually, it is reported that convection and thermophoresis are generated during optical trapping in some situations.[16–18] The flow of dissolved air is also induced inside the bubbles according to the water flow at the surrounding interface. We infer that these air and water flows and the accompanying fluidic force keep air bubbles at the specific positions near water surface (Fig. 5d).[19,20] When the laser is turned off, the elevated temperature is gradually decreased, and air solubility is recovered. Namely, the bubbles should be dissolved in water again with accompanying the decrease in their size.[21] Nevertheless, the bubble was continuously extended and then disappeared suddenly. We consider that the bubble is released to the upper air layer through disruption of the fluidic force balance.

Different from pure water, the movement of bubbles toward the surrounding was observed in the L-Phe H_2O solution during laser irradiation. Considering the results that the behavior of bubbles was varied depending on laser power and L-Phe and D_2O concentrations, the bubble movement prior to the crystallization implies that the solution state was changed during the irradiation. In the L-Phe solution, optical trapping of the liquid-like clusters should be induced in competitive manner with the bubble generation. In our previous study using the higher concentration L-Phe solutions, we proposed that optical trapping of the clusters gives a highly concentrated dense cluster domain prior to

the crystallization.[3] We consider that the cluster domain formation is responsible for the bubble movement toward the surrounding. The laser irradiation gathers the clusters, and concentration in the focal volume is increased (Fig. 5e). Once liquid nucleation is induced, the small cluster dense domain is extended to the outside of the focus. The dense domain formation would vary temperature, surface tension, L-Phe concentration, and solution viscosity. As the result, the bubbles move away from the focus (Fig. 5f). When crystal nucleation is induced in the dense domain, the formed crystal grows continuously under laser irradiation in the manner similar to the higher concentration solutions (Fig. 5g, 5f).[3] We infer that, in the samples showing crystallization without bubbles, optical trapping of the clusters is efficiently induced at the early stage of the irradiation and the bubble generation is suppressed with a dense cluster domain (Fig. 5i, 5j). Both bubble generation and cluster domain formation are nucleation phenomena with stochastic nature. They are induced competitively under the laser irradiation into the L-Phe H_2O solution, stochastically leading to the route of Fig. 5c–5f or Fig. 5i–5j.

In conclusion, we observed bubble generation outside the focus upon the irradiation of the focused 1064-nm cw laser into surface of water and L-Phe H_2O solution. In the former, bubbles stayed at positions distant from the focus during the irradiation, and their size and location were controllable by laser power. We discussed these behaviors from the viewpoint of temperature elevation accompanying the decrease in air solubility. In the latter, bubbles move toward the surrounding, and subsequently crystallization took place at the focus. We explained that the movement of bubbles is due to the formation of a dense cluster domain. Namely, this is the first observation of the formation of the crystal precursor state using a probe in laser trapping-induced crystallization. The air bubbles in this study will be possibly used to manipulate various nanomaterials as demonstrated previously with the use of a vapor bubble.[6–9] Since the air bubbles are formed at temperature below the boiling point of water, the manipulation can be carried out under relatively mild condition. Furthermore, we believe that the present bubble generation is interesting and important as the mechanistic study of laser trapping-induced crystallization.

Acknowledgments

The present work is partly supported by the Center for Emergent Functional Matter Science of National Chiao Tung University from The Featured Areas Research Center Program within the framework of the Higher Education SPROUT Project by the Ministry of Education (MOE) in Taiwan. Thanks are also due to the Ministry of Science and Technology (MOST) in Taiwan (MOST 106-2113-M-009-017- to T.S. and MOST 107-3017-F-009-003 to H.M.) and JSPS KAKENHI Grant Number JP16H06507 in Scientific Research on Innovative Areas “Nano-Material Optical-Manipulation” to T.S. and JP17K14427 for Young Scientists (B) to K.Y.

References

1) A. Ashkin, Proc. Natl. Acad. Sci. USA **94**, 4853 (1997).
2) T. Sugiyama, K. Yuyama, and H. Masuhara, Acc. Chem. Res. **45**, 1946 (2012).
3) K. Yuyama, J. George, K. G. Thomas, T. Sugiyama, and H. Masuhara, Cryst. Growth Des. **16**, 953 (2016).
4) S.-F. Wang, K. Yuyama, T. Sugiyama, and H. Masuhara, J. Phys. Chem. C **120**, 15578 (2016).
5) T. Kudo, S.-F. Wang, K. Yuyama, and H. Masuhara, Nano Lett. **16**, 3058 (2016).
6) S. Fujii, K. Kobayashi, K. Kanaizuka, T. Okamoto, S. Toyabe, E. Muneyuki, and M. Haga, Chem. Lett. **39**, 92 (2010).
7) T. Uwada, S. Fujii, T. Sugiyama, A. Usman, A. Miura, H. Masuhara, K. Kanaizuka, and M. Haga, ACS Appl. Mater. Interfaces **4**, 1158 (2012).
8) S. Fujii, K. Kanaizuka, S. Toyabe, K. Kobayashi, E. Muneyuki, and M. Haga, Langmuir **27**, 8605 (2011).
9) B. Roy, M. Arya, P. Thomas, J. K. Jürgschat, K. V. Rao, A. Banerjee, C. M. Reddy, and S. Roy, Langmuir **29**, 14733 (2013).
10) Y. Zheng, H. Liu, Y. Wang, C. Zhu, S. Wang, J. Cao, and S. Zhu, Lab Chip **11**, 3816 (2011).
11) T. M. Burns, D. Preece, T. A. Niemenen, and H. Rubinsztein-Dunlop, Proc. SPIE **8810**, 88102B (2013).
12) Y. Nishimura, K. Nishida, Y. Yamamoto, S. Ito, S. Tokonami, and T. Iida, J. Phys. Chem. C **118**, 18799 (2014).
13) K. Setoura, S. Ito, and H. Miyasaka, Nanoscale **9**, 719 (2017).
14) S. Ito, T. Sugiyama, N. Toitani, G. Katayama, and H. Miyasaka, J. Phys. Chem. B **111**, 2365 (2007).
15) R. C. Weast, *CRC Handbook of Chemistry and Physics 1st Student Edition* (CRC Press, Inc., Florida, 1988), p. B-332.
16) O. A. Louchev, S. Juodkazis, N. Murazawa, S. Wada, and H. Misawa, Opt. Exp. **16**, 5673 (2008).
17) K. Yuyama, T. Rungsimanon, T. Sugiyama, and H. Masuhara, J. Phys. Chem. C **116**, 6809 (2012).
18) T. Shoji, J. Saitoh, N. Kitamura, F. Nagasawa, K. Murakoshi, H. Yamauchi, S. Ito, H.

Miyasaka, H. Ishihara, and Y. Tsuboi, J. Am. Chem. Soc. **135**, 6643 (2013).

19) J.-P. Delville, M. Robert de Saint Vincent, R. D. Schroll, H. Chraïbi, B. Issenmann, R. Wunenburger, D. Lasseux, W. W Zhang, and E. Brasselet, J. Opt. A: Pure Appl. Opt. **11**, 034015 (2009).
20) A. Diguet, R.-M. Guillermic, N. Magome, A. Saint-Jalmes, Y. Chen, K. Yoshikawa, and D. Baigl, Angew. Chem., Int. Ed. **48**, 9281 (2009).
21) G. Baffou, J. Polleux, H. Rigneault, and S. Monneret, J. Phys. Chem. C **118**, 4890 (2014).

Figure Captions

Fig. 1. Optical micrographs upon the laser irradiation into solution surface of H_2O. Irradiation time and laser power are shown in each image. Green arrows indicate bubbles outside the focal spot, and small black dots are artifacts due to contamination in optical items. The focal spot is indicated with a star-shaped mark. Line profiles of some bubbles are inserted in the images. The image size is 220 μm in width and 180 μm in height.

Fig. 2. (a) Optical micrographs upon switching off the laser. Time after turning off the laser is given in each image. The image size is 35 μm in width and 35 μm in height. (b) The temporal change in the diameter of the bubble estimated from the EMCCD images.

Fig. 3. Optical micrographs upon the laser irradiation at 1.1 W into solution surface of the L-Phe H_2O solution. Irradiation time is shown in each image. Green arrows indicate bubbles. The image size is 80 μm in width and 60 μm in height.

Fig. 4. The times required for (a) the bubble movement and (b) the crystallization. (c) The relation between the time for the bubble movement and the crystallization time.

Fig. 5. The schematic illustration of possible mechanism for the bubble generation. The bubble generation summarized in upper figures is observed in common for water and L-Phe H_2O solution, while the behavior in lower figures is specific for the latter sample.

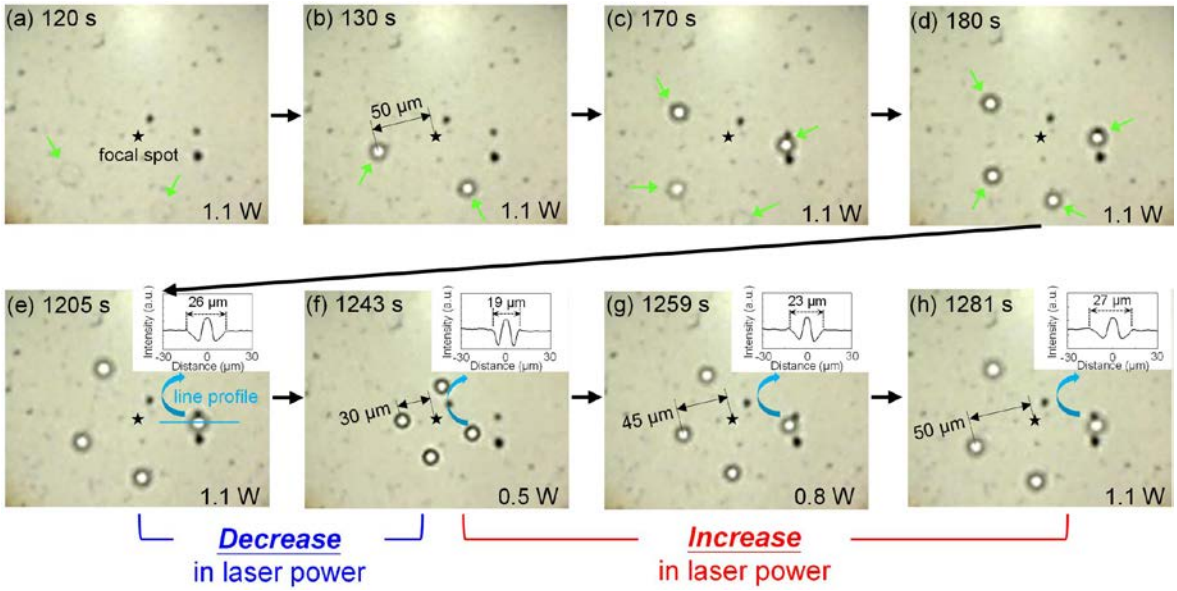
(a) 120 s
focal spot
1.1 W
(b) 130 s
50 μm
1.1 W
(c) 170 s
1.1 W
(d) 180 s
1.1 W
(e) 1205 s
26 μm
line profile
1.1 W
(f) 1243 s
19 μm
30 μm
0.5 W
(g) 1259 s
23 μm
45 μm
0.8 W
(h) 1281 s
27 μm
50 μm
1.1 W
Decrease
in laser power
Increase
in laser power

Fig.1.

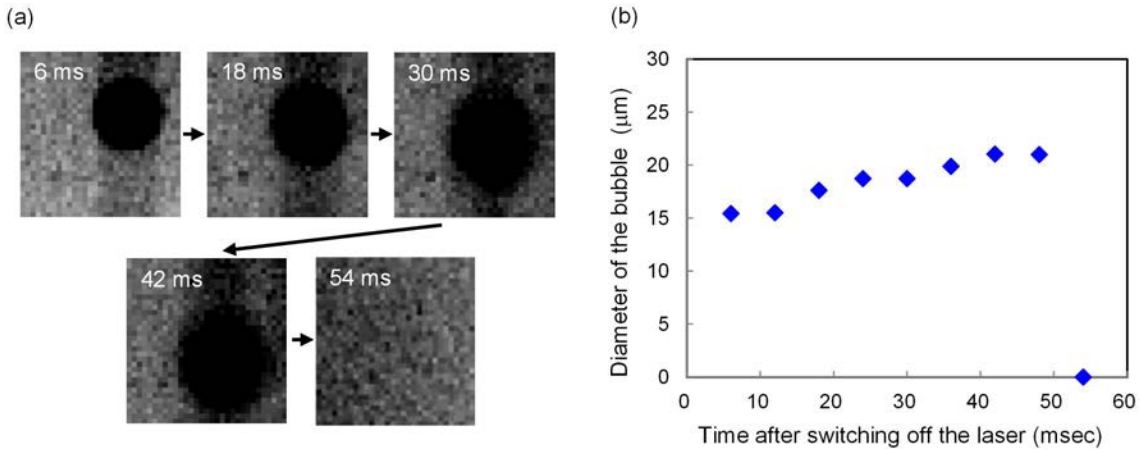
(a)
6 ms
18 ms
30 ms
42 ms
54 ms
(b)
Diameter of the bubble (μm)
0
5
10
15
20
25
30
0
10
20
30
40
50
60
Time after switching off the laser (msec)

Fig. 2.

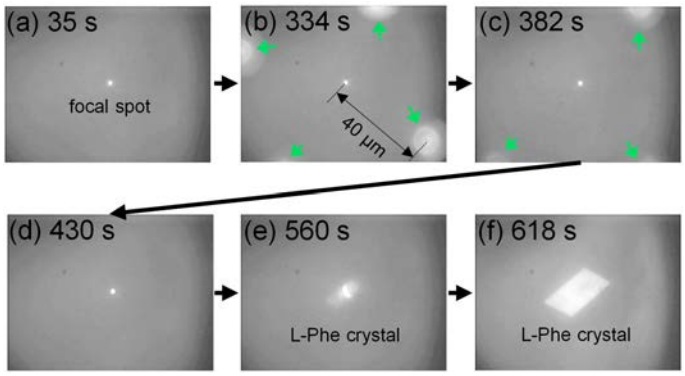
(a) 35 s
focal spot
(b) 334 s
40 μm
(c) 382 s
(d) 430 s
(e) 560 s
L-Phe crystal
(f) 618 s
L-Phe crystal

Fig. 3.

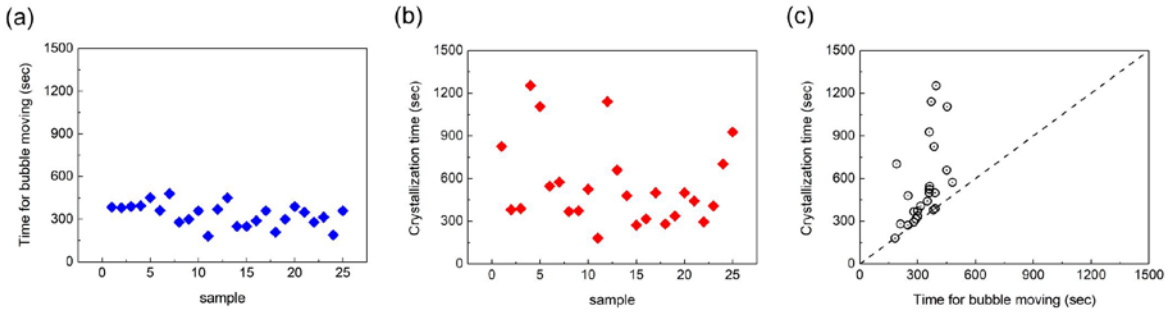
(a)
Time for bubble moving (sec)
sample
(b)
Crystallization time (sec)
sample
(c)
Crystallization time (sec)
Time for bubble moving (sec)

Fig. 4.

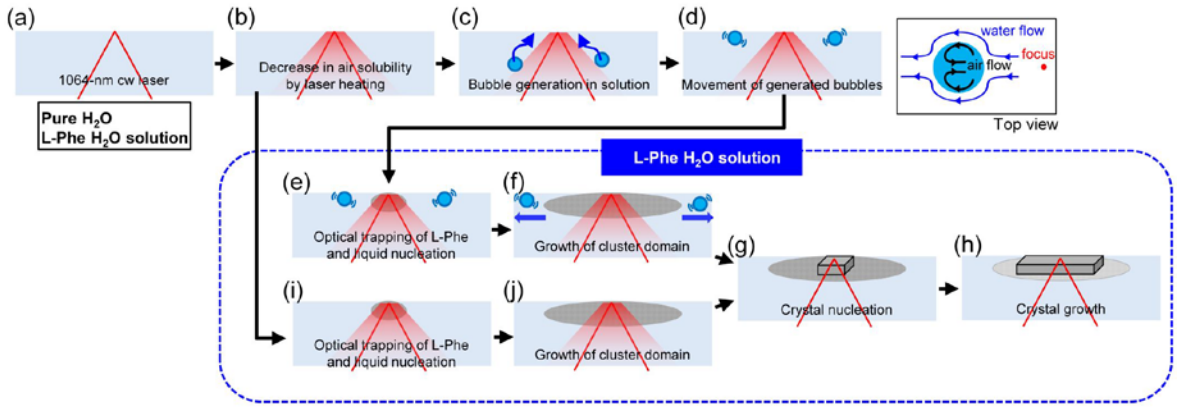
(a)
1064-nm cw laser
Pure H2O
L-Phe H2O solution
(b)
Decrease in air solubility by laser heating
(c)
Bubble generation in solution
(d)
Movement of generated bubbles
water flow
focus
air flow
Top view
L-Phe H2O solution
(e)
Optical trapping of L-Phe and liquid nucleation
(f)
Growth of cluster domain
(g)
Crystal nucleation
(h)
Crystal growth
(i)
Optical trapping of L-Phe and liquid nucleation
(j)
Growth of cluster domain

Fig. 5.